Transport studies in H_3PO_4-doped polyaniline

J. F. Rouleau, J. Goyette, and T. K. Bose
Institut de Recherche sur l'Hydrogène, Département de Physique, Université du Québec à Trois-Rivières, Case Postale 500 Trois-Rivières, Québec, Canada G9A 5H7

R. Singh and R. P. Tandon
National Physical Laboratory, Dr. K. S. Krishnan Road, New Delhi, 110012, India
(Received 20 January 1995; revised manuscript received 10 April 1995)

An experimental study of the temperature and frequency dependence (in the audio and rf and microwave regions) of the conductivity of H_3PO_4-doped polyaniline samples is presented. The dopant concentration of the samples varies between $0.09M$ and $3.60M$. For all the samples studied, the temperature dependence of the dc conductivity is consistent with the expression for Mott's variable-range hopping. On the other hand, in the temperature range $88 \leq T \leq 298$ K and in the audio frequency range 20 Hz $\leq f \leq 1$ MHz, we remark that the ac conductivity (σ_{ac}) does not vary much with frequency. From our wide-band measurement in the microwave region, however, we find that, for the $0.09M$-doped sample, σ_{ac} varies as ω^s with $s \cong 0.6$; using Mott's model for the hopping conduction in the ac regime, we find that this value of s yields a reasonable estimation for the hopping probability: $\nu_{ph} \sim 6.92 \times 10^{13}\ s^{-1}$.

I. INTRODUCTION

A number of investigations undertaken in the past to study the conducting properties in polymers such as polyacetylene, polypyrrole, etc.[1,2] have contributed to highlight conduction processes in such materials. Recently, the polyaniline family of polymers has also been the subject of increased investigation because its electronic properties can be modified by protonation, giving rise to unusual chemical, optical, electrochromic, and electrical properties both in insulating and conducting forms.[3] Several possible applications have attracted attention, such as electromagnetic interference shielding, lightweight batteries, conducting wires, electrochromic devices, sensors, and, more recently, optical computing, just to mention a few.[4,5]

Polyaniline (referred to as PAN) is structurally quite different from the other known conducting polymers. Its backbone structure is composed of nitrogen atoms occupying the bridging positions between carbon rings. As these nitrogen atoms are at the same time the protonation sites, there is a strong possibility of protonation-induced modifications of the electronic properties. In fact, it has been demonstrated that a dramatic increase of 11 orders of magnitude in conductivity (insulator-conductor transition) in emeraldine can be caused by a protonation process called acid doping.[6] It has been shown that electrochemical doping can be used to induce insulator-to-conductor transition. The ultimate electrical properties of PAN will therefore be governed by the method of preparation, doping level, and oxidation state.

Band-structure calculations for protonated PAN (Refs. 7 and 8) reveal highly asymmetric valence and conduction bands with only a half occupied polaron band deep into the gap as opposed to the usual two bands in a normal conducting polymer. This half-filled polaron band is the cause of some metallic properties such as Pauli's magnetic susceptibility, a small value of thermopower linearly decreasing with temperature, and free-carrier absorption, all typical of a metal.[9,10]

In the present work, we have carried out experiments on H_3PO_4-doped PAN. This particular dopant causes substantial changes in the conductivity which could be investigated to understand the mechanism of conduction. Our measurements were done over a wide band of frequencies in the audio and rf and microwave regions in order to study both the dc and ac conductivities.

II. EXPERIMENTAL TECHNIQUES

The emeraldine base was chemically prepared from a mixture of aniline and HCl, to which was added a second solution of ammonium persulfate $(NH_4)_2S_2O_8$. A brownish precipitate was obtained and was then treated with a known volume and concentration of H_3PO_4 to achieve the desired doping level. Figure 1 shows the molecular structure of the emeraldine base and the two possible configurations of the doped PAN. The dried powders were compacted under a pressure of 100 MPa to form pill-shaped samples having a radius of about 8 mm and a height of 2 mm. Before each measurement, the samples were dried again in order to eliminate the effects of absorbed water.

The dielectric properties of the samples were measured in the rf and microwave frequency range (50 MHz to 5 GHz) using a network analyzer (HP8510B) fed by a synthesizer (HP8341). The probe used was an open-ended 7-mm coaxial line cut flat and put in direct contact with the sample under study. At each frequency, the real (ε') and imaginary (ε'') parts of the permittivity are given by the bilinear relation[11]

$$\varepsilon' - j\varepsilon'' = \frac{\Gamma A + B}{\Gamma + C}\ , \tag{1}$$

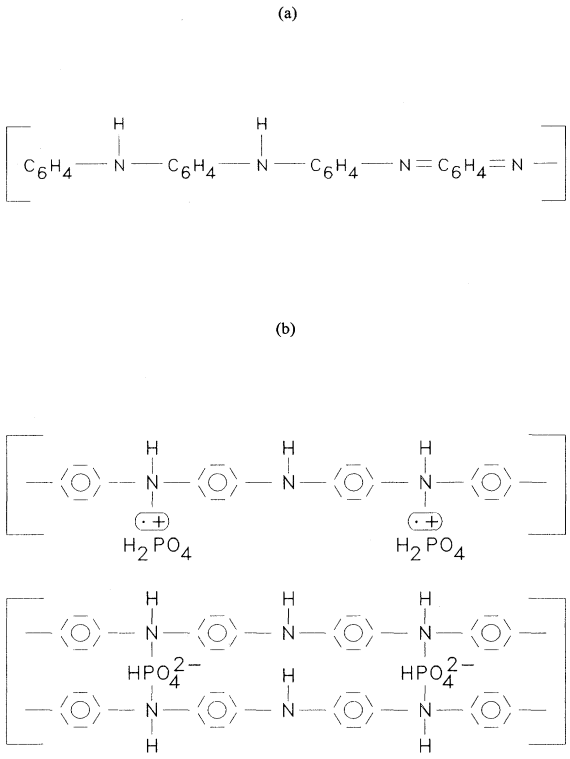

FIG. 1. Molecular structure of (a) the emeraldine base and (b) the two possible molecular configurations of the doped PAN (H_3PO_4).

where Γ is the measured complex reflection coefficient of the probe sample system and A, B, and C are complex constants found from a calibration made with three known dielectrics (in our case, air, methanol, and mercury). This technique has two distinct advantages. First, the measurements are performed on electrodeless samples, which rules out any spurious effects. Second, they are made over a rather large frequency range, unlike the conventional cavity perturbation technique, which provides fixed frequency values only. The total measured conductivity is computed from the relation

$$\sigma_m(\omega)=\mathrm{Re}\{j\omega\varepsilon^*\}=\omega\varepsilon'' \ . \tag{2}$$

After the completion of the measurements in the rf and microwave regions, the samples were covered with silver paint (GE Electronics, USA) to act as electrodes, and our low-frequency measurements were carried out with an impedance analyzer (HP4284A) and a three-terminal cell. The temperature and frequency dependence of the complex permittivity and conductivity were then computed from the measured parallel combination of the conductance and susceptance of our pill-shaped samples.

III. EXPERIMENTAL RESULTS

At room temperature, undoped samples of PAN have a dc conductivity of the order of 10^{-9} S/cm.[12] The measured conductivity of the doped samples we have studied varies between 10^{-7} and 10^{-1} S/cm; our measurements show that, for each sample, the conductivity increases quite sharply with the temperature and somewhat less with the frequency. Moreover, the conductivity increases with the doping level for the first seven samples (0.09M, 0.72M, 0.90M, 1.08M, 1.35M, 1.44M, and 1.80M), reaching a maximum at 1.80M and decreasing for the last sample (3.60M). We will discuss these results in more detail.

A. Temperature dependence of the dc conductivity

We have measured the dc conductivity over a rather wide temperature range of $88<T<298$ K. We took as dc conductivity the conductivity measured at a frequency of 20 Hz. We feel justified in doing so, since, at that frequency and up to at least 1 kHz, the measured conductivity did not show any significant variation with frequency for all the samples studied (see Fig. 2, which is typical of the behavior of all the samples). We can also remark that our values of the dc conductivity in PAN are of the same magnitude as the one reported for polypyrrole.[2]

A rough picture of conducting polymers would be to consider that they are disordered materials formed basically of one-dimensional chains. Depending on if the electronic states of such a material remain fairly well localized near the chains or if they overlap over neighboring chains, the conductivity will be one (1D) or three dimensional. A mechanism very often proposed to explain the dc conductivity in disordered and amorphous materials is Mott's variable-range hopping.[13] According to this model, the conductivity should vary as[14]

$$\sigma_{\mathrm{dc}}=\sigma_0\exp\left[-\left[\frac{T_0}{T}\right]^{1/(1+d)}\right], \tag{3}$$

where d is the dimensionality of the conduction process and T_0 a constant. So, it seems that it is possible to

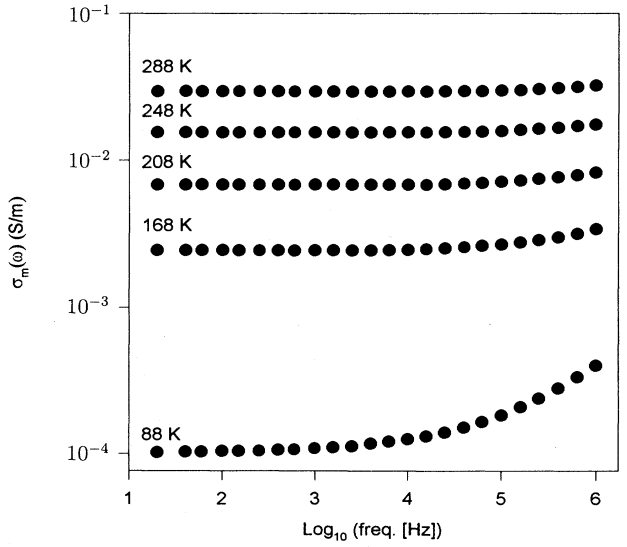

FIG. 2. Frequency dependence of the total measured conductivity for the 0.09M-doped sample.

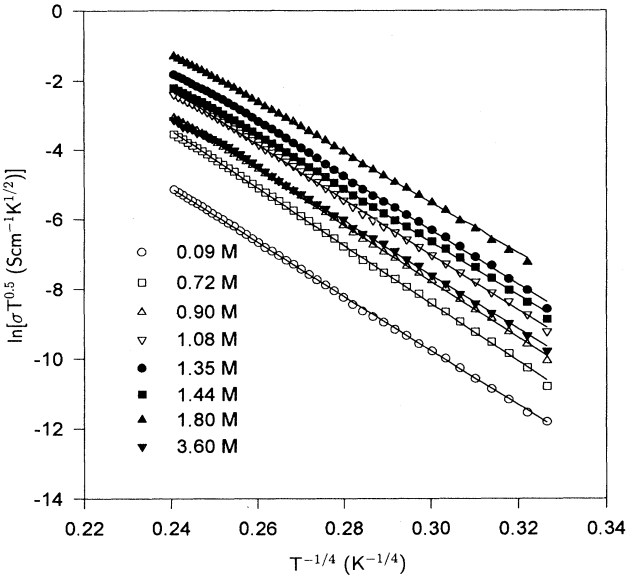

FIG. 3. Temperature dependence of the dc conductivity for all the samples.

determine whether the conductivity is 1D or 3D by studying the temperature dependence of σ_{dc}. Three-dimensional conductivity was first observed in rf-sputtered amorphous films of germanium and silicon which had been carefully annealed.[15] It has also been reported in amorphous silicon carbide films.[16] The 3D Mott's model has now been observed in many conducting polymers.[17,18] The best fit of our data to Eq. (3) is achieved by considering $d=3$. For 3D variable-range hopping the constants are given by

$$\sigma_0 = e^2 \left[\frac{9N(E_F)}{8\pi\alpha k_B T} \right]^{1/2} \nu_{ph} , \tag{4}$$

$$T_0 = \lambda\alpha^3/k_B N(E_F) , \tag{5}$$

where e is the electronic charge, $N(E_F)$ is the density of states at the Fermi energy E_F, α is the inverse of the delocalization length, ν_{ph} is a hopping frequency (estimated in the next section), k_B is the Boltzmann constant, and, finally, $\lambda \sim 18.1$ is a constant.[15,19] Two other parameters can also be defined: the average hopping distance R and the average hopping energy W which are given by[16]

$$R = \left[\frac{9}{8\pi k_B T N(E_F)} \right]^{1/4} \tag{6}$$

and

$$W = 3/4\pi R^3 N(E_F) . \tag{7}$$

If we plot a graph of $\ln(\sigma\sqrt{T})$ as a function of $T^{-1/4}$ we will get a straight line, and can find T_0 as the slope and σ_0 as the intercept of that line (see Fig. 3). Once we know these values and ν_{ph} has been evaluated (see next section), we can compute $N(E_F)$ and α from the above equations:

$$N(E_F) = (1.996\times10^{48}/\nu_{ph}^3)[(\sigma_0\sqrt{T})^3\sqrt{T_0}] \text{ cm}^3\text{ eV}^{-1} \tag{8}$$

and

$$\alpha = (21.22\times10^{13}/\nu_{ph})[(\sigma_0\sqrt{T})\sqrt{T_0}] \text{ cm}^{-1} . \tag{9}$$

Table I gives the values of the parameters found from the analysis of our dc conductivity data. One can see from Table I that our polyaniline samples have, in general, higher $N(E_F)$ values than these obtained by Singh *et al.* for polypyrrole.[2] This can be explained to some extent by the fact that our samples show a higher conductivity.

B. Frequency dependence of the conductivity

The ac conductivity is defined as

$$\sigma_{ac}(\omega) = \sigma_m(\omega) - \sigma_{dc} , \tag{10}$$

where $\sigma_m(\omega)$ is the total measured conductivity (ac and dc parts). In the low-temperature region, it is expected that the general behavior of $\sigma_{ac}(\omega)$ can be described by the relation[20]

$$\sigma_{ac}(\omega) = A\omega^s , \tag{11}$$

where s does not vary much with temperature. Figure 2 shows the variation of the total measured conductivity for the 0.09M sample in the audio region. Although the frequency-dependent conductivity becomes more visible at low temperatures, the audio frequency data even at low temperatures are not sufficient to deduce a precise value of s.

However, we have also made measurements of the mi-

TABLE I. Parameters found from a fit of our data to Eq. (3).

Doping level (M)	$\sigma_0\sqrt{T}$ (10^3S cm^{-1} K$^{0.5}$)	T_0 (10^7 K)	α (10^{10} cm^{-1})	$N(E_F)$ (cm^{-3}eV^{-1})	R (10^{-10} cm)	W (eV)	αR
0.09	0.76±0.06	3.64±0.06	0.0014±0.0002	(1.6±0.7)×10^{19}	5950±675	0.071±0.039	8.3±1.5
0.72	13.8±1.0	4.71±0.06	0.029±0.004	(1.1±0.4)×10^{23}	306±33	0.076±0.040	8.8±1.5
0.90	12.7±0.9	4.19±0.06	0.025±0.003	(8.0±2.9)×10^{22}	342±32	0.074±0.034	8.6±1.3
1.08	18.4±1.3	3.92±0.05	0.035±0.005	(2.3±0.9)×10^{23}	241±27	0.073±0.039	8.5±1.5
1.35	23.3±2.2	3.62±0.06	0.042±0.006	(4.6±1.9)×10^{23}	193±21	0.072±0.038	8.3±1.4
1.44	11.1±0.9	3.38±0.05	0.019±0.003	(4.8±2.1)×10^{22}	413±49	0.071±0.040	8.1±1.5
1.80	9.9±0.1	2.69±0.05	0.015±0.002	(3.1±1.1)×10^{22}	489±49	0.067±0.032	7.7±1.2
3.60	5.6±0.6	3.54±0.07	0.010±0.002	(6.4±3.6)×10^{21}	808±123	0.071±0.049	8.2±2.0

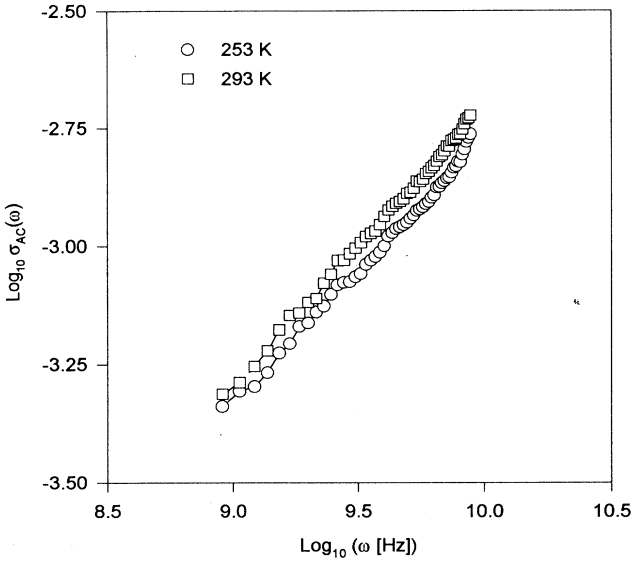

FIG. 4. Frequency dependence of the ac conductivity at $T=253$ and 293 K for the 0.09M-doped sample.

crowave conductivity of our samples in the frequency range 50 MHz to 5 GHz over a smaller temperature range (253–303 K). The total measured conductivity is computed directly from the measured dielectric loss ε'' and $\sigma_{ac}(\omega)$ is found by subtracting the dc conductivity from the total conductivity. Figure 4 depicts the frequency dependence of $\sigma_{ac}(\omega)$ at two different temperatures for the 0.09M sample, and Table II gives the value of the exponent s that we were able to compute from the slope of these graphs. It turns out to be ~ 0.6 within experimental errors. Mott's model for the hopping conduction in the ac regime[13] links the exponent s to the phonon frequency ν_{ph}:

$$s = 1 - \frac{4}{\ln(\nu_{ph}/\omega)} . \tag{12}$$

Therefore, our knowledge of s permits us to estimate the value of ν_{ph} that we need in order to compute $N(E_F)$ and α [Eqs. (8) and (9)]. The exponent s is more difficult to estimate for higher level of dopant because the ac conductivity becomes quite small relative to the dc conductivity.

TABLE II. Computed values of s from Eq. (11) for the 0.09M doped sample. The error corresponds to three standard deviations.

Exponent	253 (K)	263 (K)	273 (K)	283 (K)	293 (K)
s	0.568	0.581	0.596	0.587	0.596
Δs	0.018	0.015	0.015	0.012	0.012

IV. DISCUSSION

We want to start this discussion by emphasizing the usefulness of the microwave data, since it helps us to evaluate the exponent s over a significant frequency range. Using Mott's hopping conduction expression for the ac regime, it is possible to compute the value of the hopping frequency ν_{ph} according to Eq. (12). A value of s of the order of 0.6 is found, and, therefore, one can estimate $\nu_{ph} \approx 6.92 \times 10^{13}$ sec^{-1}, which is close to the value observed in amorphous solids[15] like Ge, Si, and polypyrrole.[17]

The temperature dependence of the dc conductivity in amorphous materials can follow many regimes. First of all, the $\ln(\sigma(T)) \propto T^{-1}$ dependence is often observed and can be related to nearest-neighbor hopping (Miller-Abrahams hopping) or to an activation-type mechanism which follows the Arrhenius behavior. Such a temperature dependence is observed mainly in the range[21] $200 < T < 300$ K. As the temperature is lowered, and, consequently, as the thermal energy $k_B T$ is decreased, the Arrhenius law fails and the conductivity follows a $\ln(\sigma(T)) \propto T^{-\alpha}$ law, where now α equals $\frac{1}{4}$ or $\frac{1}{2}$. Temperature dependence of this type has been observed at temperatures[18,22] down to $T \cong 10$ K and is consistent with both 1D ($\alpha = \frac{1}{2}$) and 3D ($\alpha = \frac{1}{4}$) variable-range hopping (VRH) models. But, on the other hand, the VRH model is not the only model which leads to $T^{-1/2}$ or $T^{-1/4}$ behavior. Some workers have explained a $T^{-1/2}$ dependence as arising either from the charging-energy limited tunneling (CELT) between metallic grains[10] or from a distribution of hopping energies due to variations in the effective conjugation length.[23] Sheng and co-workers[24,25] have proposed a model for a granular system involving tunneling of electrons and holes from the charged sites to neutral sites, yielding also a $T^{-1/2}$ dependence over a wide range of temperature with a crossover to $T^{-1/4}$ behavior at low temperature.

We feel, nevertheless, justified in analyzing our data in terms of the variable-range hopping model. First, the best fit to our dc conductivity data was achieved when we consider $d=3$ in Eq. (3). Moreover, as it can be seen from Table I, reasonable values of σ_0 and T_0 can be found when we assume that the conduction is three dimensional and that it follows the VRH model; our estimates of $N(E_F)$ and other parameters found from the $\ln(\sigma_{dc})$ vs $T^{-1/4}$ plots show that Mott's law remains applicable for quite high doping level. It may be pointed out also that the present results, where αR is around 8 and $W \sim 4$ kT, are quite consistent with Mott's requirements that αR should be comparable to 1 and W to kT in order to have hopping to distant sites. As mentioned before, Mott's VRH model has already found widespread use in the case of amorphous semiconductors and doped polyacetylene, and it is not surprising that it can also be used with doped PAN.

Let us point out that the findings of other workers are consistent with our use of the 3D-VRH model. Zuo *et al.*[10] initially used the CELT model to explain doped PAN properties. On the other hand, in a more recent paper, Wang *et al.*[26] seem to demonstrate the validity of

the 1D-VRH model. Recently, however, Zuo *et al.*[18] observed a 3D-VRH mechanism occurring in HCl-doped PAN for lowly protonated samples ($y < 0.13$) over the temperature range $88 < T < 300$ K. Whether the conductivity follows a 1D behavior (or quasi-1D) or a 3D behavior depends mostly on interchain coupling, since a strong coupling will inhibit 1D electron localization. In that sense, Wang *et al.*[27] have suggested that the emeraldine salt form of PAN can be classified as a quasi-1D disordered conductor composed of bundles of coupled parallel chains in which the electron wave functions are 3D delocalized. More recently, Misurkin *et al.*[28] have even proposed that PAN is a 3D system which is composed of finite conjugated fragments. According to that model, if this delocalization occurs over the entire sample, that is, if electron hopping takes place for all those metallic islands or fragments in the sample, then the conductivity should follow a $\ln(\sigma) \propto T^{-1/4}$ law.

Let us conclude by saying that the explanation of the conduction mechanisms in doped PAN is not definitive. Even though arguments made on the basis of our data can support the VRH model, we certainly cannot exclude other conduction mechanisms having a temperature dependence similar to 3D-VRH.

ACKNOWLEDGMENTS

We would like to thank Dr. Pierre Bénard for valuable discussion. This research was carried out with grants from NSERC, Canada. One of us (J.F.R.) would like to thank NSERC for financial support.

[1]C. K. Chiang, C. R. Fincher, Jr., Y. W. Park, and A. J. Heeger, Phys. Rev. Lett. **39**, 1098 (1977).
[2]R. Singh, R. P. Tandon, V. S. Panwar, and S. Chandra, J. Appl. Phys. **69**, 2504 (1991).
[3]P. M. McManus, S. C. Yang, and R. J. Cushman, J. Chem. Soc. D **1985**, 1556.
[4]A. J. Epstein and A. G. MacDiarmid, *Industrial Workshop Science and Application of Conducting Polymers,* Proceedings of the European Physical Society, Lofthus, Norway, 1990 (Hilger, Bristol, 1991).
[5]A. J. Epstein and A. G. MacDiarmid, Makromol. Chem. Macromol. Symp. **51**, 217 (1991).
[6]E. M. Geniés, A. Boyle, M. Lapkowski, and C. Tsintaris, Synth. Met. **35**, 139 (1990).
[7]A. P. Monkman, D. Bloor, G. C. Stevens, and J. C. H. Stevens, J. Phys. D **20**, 1337 (1987).
[8]S. Stafström, J. L. Brédas, A. J. Epstein, H. S. Woo, D. B. Tanner, W. S. Huang, and A. G. MacDiarmid, Phys. Rev. Lett. **59**, 1464 (1987).
[9]J. M. Ginder, A. F. Richter, A. G. MacDiarmid, and A. J. Epstein, Solid State Commun. **63**, 97 (1987).
[10]F. Zuo, M. Angelopoulos, A. G. MacDiarmid, and A. J. Epstein, Phys. Rev. B **36**, 3475 (1987).
[11]R. Nozaki and T. K. Bose, IEEE Trans. Instrum. Meas. **39**, 945 (1990).
[12]H. H. S. Javadi, K. R. Cromack, A. G. MacDiarmid, and A. J. Epstein, Phys. Rev. B **39**, 3579 (1989).
[13]N. F. Mott and E. A. Davis, *Electronic Processes in Noncrystalline Materials* (Clarendon, London, 1979).
[14]W. Brenig, G. H. Döhler, and H. Heyszenau, Philos. Mag. **27**, 1093 (1972).
[15]D. K. Paul and S. S. Mitra, Phys. Rev. Lett. **31**, 1000 (1973).
[16]K. Nair and S. S. Mitra, J. Non-Cryst. Solids **24**, 1 (1977).
[17]R. Singh, R. P. Tandon, and S. Chandra, J. Appl. Phys. **70**, 243 (1991).
[18]F. Zuo, M. Angelopoulos, A. G. MacDiarmid, and A. J. Epstein, Phys. Rev. B **39**, 3570 (1989).
[19]C. H. Seager and G. E. Pike, Phys. Rev. B **10**, 1435 (1974).
[20]A. R. Long, Adv. Phys. **31**, 553 (1982).
[21]R. Pelster, G. Nimtz, and B. Wessling, Phys. Rev. B **49**, 12 718 (1994).
[22]Z. H. Wang, H. H. S. Javadi, A. Ray, A. G. MacDiarmid, and A. J. Epstein, Phys. Rev. B **42**, 5411 (1990).
[23]L. W. Shacklette and R. H. Baughman, Mol. Cryst. Liq. Cryst. **189**, 193 (1990).
[24]P. Sheng and B. Abeles, Phys. Rev. Lett. **28**, 34 (1972).
[25]P. Sheng and J. Klafter, Phys. Rev. B **27**, 2583 (1983).
[26]Z. H. Wang, E. Ehrenfreund, A. Ray, A. G. MacDiarmid, and A. J. Epstein, Mol. Cryst. Liq. Cryst. **189**, 263 (1990).
[27]Z. H. Wang, C. Li, E. M. Scherr, A. G. MacDiarmid, and A. J. Epstein Phys. Rev. Lett. **66**, 1745 (1991).
[28]I. A. Misurkin, T. S. Zhuravleva, V. M. Geskin, V. Gulbinas, S. Pakalnis, and V. Butvilos, Phys. Rev. B **49**, 7178 (1994).